We are IntechOpen,
the world's leading publisher of
Open Access books
Built by scientists, for scientists

6,900
Open access books available

186,000
International authors and editors

200M
Downloads

Our authors are among the

154
Countries delivered to

TOP 1%
most cited scientists

12.2%
Contributors from top 500 universities

CLARIVATE ANALYTICS
BOOK CITATION INDEX
INDEXED

WEB OF SCIENCE™

Selection of our books indexed in the Book Citation Index
in Web of Science™ Core Collection (BKCI)

Interested in publishing with us?
Contact book.department@intechopen.com

Numbers displayed above are based on latest data collected.
For more information visit www.intechopen.com

Application of Positron Annihilation Spectroscopy Studies of Bismuth and Subsurface Zone Induced by Sliding

Jerzy Dryzek

Additional information is available at the end of the chapter

Abstract

The positron annihilation, experimental and theoretical results obtained for bismuth are presented, mainly concerning the open volume defects created during compression and dry sliding. Positron lifetime in vacancy clusters increases with the size of the cluster; however, it saturates at the value of about 0.42 ns already for six vacancies in a cluster. Similar values were resolved in the positron lifetime spectra of bismuth samples exposed to dry sliding. Detection of the subsurface zone in bismuth exposed to dry sliding reveals exponential decay of vacancy clusters concentration with the depth increase from the worn surface. The high strain of about 70% was evaluated in the layer adjoined the worn surface The temperature of recrystallization obtained from the isochronal measurements of annihilation line shape parameter was equal about 90°C, and the activation energy for grain migration is about 0.84 ± 0.11 eV.

Keywords: bismuth, positron annihilation, defects, subsurface zone

1. Introduction

The technological processes like machining, polishing, sandblasting, and sliding or more sophisticated, i.e., laser treatments or ion implantations not only affect the surface of the material but also modify the subsurface region below it changing its physical properties. This is due to the elastic and plastic deformation, which expands into the interior. In the literature, a zone adjoining the surface which properties are changed due to sliding or friction is called work hardening zone because an increase in hardness is apparent [1]. Nevertheless,

some changes expand deeper and the whole region affected we called the subsurface zone [2]. Generation of the subsurface zone is inherent in any surface treatment.

When two bodies are in a sliding contact, a load at their surfaces is supported by asperities of the rough solid surfaces [3]. The asperities deform through elastic and plastic modes, increasing the contact area between the two surfaces until the contact area is sufficient to support the load. High-stress concentration in these regions can lead to a damage and thus also the crack initiation [4]. The asperity region is the source of dislocations that are driven introducing the stress concentration in the subsurface zone [5]. It is not excluded that a great number of small impacts on the worn surface force propagate deformation at large distances into the interior [6] and is the deformation is observed at depth of hundreds of micrometers from the surface [7].

One can indicate several layers in the subsurface zone, **Figure 1**. Directly on top is a layer of contamination, then an adsorption layer and a deeper reaction layer with oxides and other compounds [1]. These layers are present at the depth of about 10 nm from the surface. Much deeper in the damage zone, with deformed grains, band shears, and other defects is extended. This zone has the thickness more than a hundred micrometers, and it seems that this is the main layer, which carries the stress induced by the load on the surface. Below, undamaged and unaffected bulk region is located. The strain and accompanied crystalline defects are distributed in the subsurface zone and they are linked with surface treatments. The most important is the friction and wear which are always present during manufacturing.

The subsurface zone is a subject of tribology; however, its existence can affect for instance electrical properties of conductors as well. Due to the skin effect, alternating electric current (AC) flows within a conductor near the surface at the depth of about 100 μm depending on the frequency and electrical properties of a conductor. This depth coincides with the subsurface
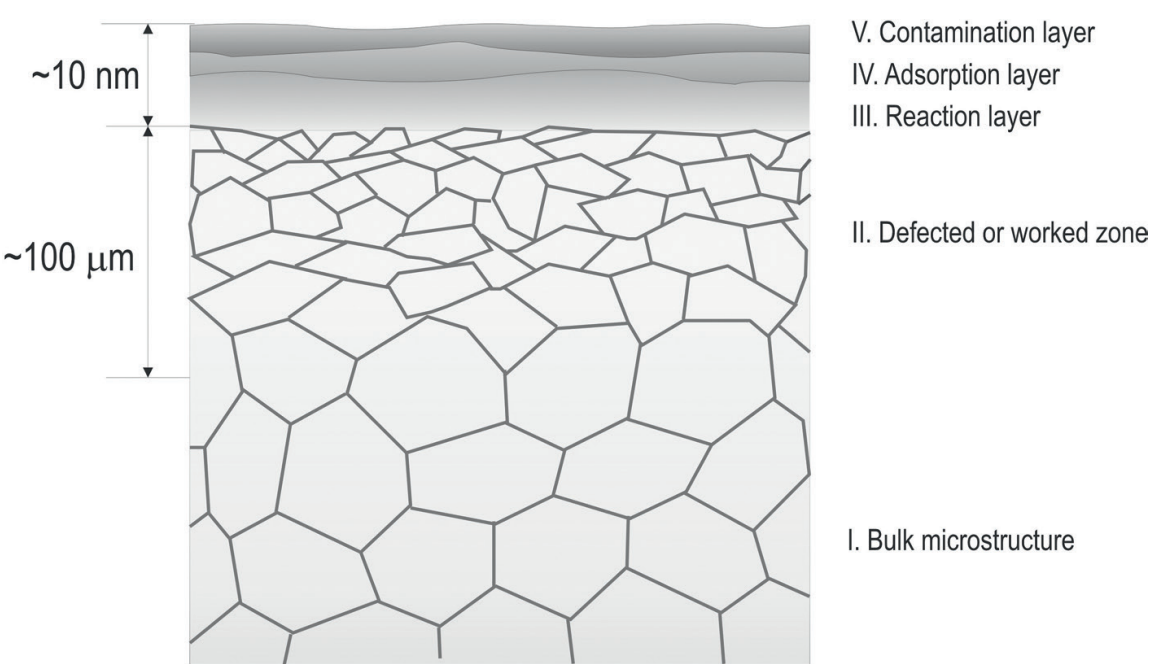

Figure 1. The schema of the subsurface region located below the worn surface (on the top).

zone depth generated during, e.g. machining or sandblasting, in copper it is about 140–800 μm as it was reported, see Ref [8]. The skin effect causes that electrons flow mainly near the surface of the conductor, but in this region, they can scatter at crystalline defects which were created during manufacturing of wires or other devices. Therefore, recently, we focused our interest on the subsurface zone in metals and alloys, which are used for the construction of the electronic devices in radio frequency techniques [9].

The experimental study of the subsurface zone is not an easy task. Measuring the depth profile of microhardness in a sample cross section is one of the methods. However, this is not a suitable method of detecting defects at the atomic level. Commonly used methods such as XRD, SEM and TEM also fail in the case of point defects, which occur in large amounts during a plastic deformation under sliding condition. Positron annihilation methods, due to the several reasons, complete the gap. Extremely sensitivity and selectivity to the open volume defects at atomic level, large positron implantation depth, they are only one of them [10]. Experiments have shown the usefulness of these methods for studies of defects and their distribution in subsurface zones.

Bismuth is a plastic semimetal, and it is not the material in tribo junctions; however, it is used as a component of several alloys, for instance, solid lubricants or recently in low friction aluminum alloy DHT-3 [11]. Low melting point of this metal, i.e., 270.8°C, allows us to suppose that this can affect the subsurface zone generation under dry sliding condition. Other positron annihilation studies of bismuth samples are also presented.

2. Outline of positron annihilation spectroscopy

After thermalization, the positron implanted into matter annihilates with an electron, emitting two photons of energy about 511 keV in almost opposite direction. Positron annihilation spectroscopy utilizes the detection of those photons. This allows us to measure the Doppler broadening of annihilation line or the positron lifetime, i.e., how long it exists in the matter. Both reflect the matter properties at the atomic level. This is because the time prior to annihilation, which an implanted positron spends in the matter depends on the local electron density [10]. Briefly, the following correlation was established theoretically and experimentally: the higher electron density in the site where a positron annihilates the lower value of its lifetime. The electron density is highest in the core region of an atom; however, a positively charged nucleus repels the positron into interstitial sites occupied by valence and conduction electrons. Electronic density is much lower in these sites, and therefore the annihilation with these electrons contributes to the positron lifetime.

The real crystalline lattice can be locally disturbed by defects, for instance, open volume defects, like vacancies or its clusters and/or dislocations. In such defects the electronic density is lower than in interstitial sites. Positrons can be localized at these defects and this causes an increase in the positron lifetime value depending on the type of defect. For instance, the lifetime of a positron trapped at monovacancy is about four-thirds of that in bulk. These values are fingerprints which can be used for defect identification as it is reported in numerous papers [12]. The positron lifetime spectroscopy application to study the matter is based on this fact.

Additionally, the measurements of the broadening of the annihilation line allow us to trace the momentum of electrons undergoing the annihilation. The momentum of the annihilating positron electron pair depends on the local electronic density too. Then any disturbance can be reflected in the broadening, and/or shape of the annihilation line. This can happen in the open volume defects, where electronic density is suppressed. Positron annihilation with such electrons causes the annihilation line is narrower than in the case of the annihilation with interstitial valence electrons in bulk. For characterization of the annihilation line shape, the value of the S-parameter is commonly used. The S parameter is defined as the ratio of the central area to the total area under the annihilation line. This parameter is extremely sensitive to the presence of open volume defects, like monovacancies or its clusters and jogs at dislocation lines, where due to their positive charge, positrons are localized. Usually, the measurements are performed using high purity germanium detector with the good energy resolution. These both experimental techniques are widely applied to study many aspects of condensed matter problems. One should also add that temperature itself does not affect the positron lifetime or S-parameter. The main reasons of the observed altering in their values are induced by structural changes: like vacancy generation, its migration or reaction with other defects, phase transition or other structural processes.

Using conventional positron sources, i.e., beta plus isotopes like [22]Na one has to take into account the positron implantation range. The fraction of positrons, which are implanted into the matter, decreases exponentially with the depth increase from the entrance surface. In the case of bismuth linear absorption coefficient for positrons emitted from [22]Na is about 569 cm^{-1}, it means about 63% positrons annihilates in the layer of the depth of about 17 μm from the entrance surface [13]. This allows to probe large region in a sample by positrons and reflects its bulk properties at the atomic scale.

3. Positron lifetime in bismuth

In our studies, all measurements were performed for the samples of pure bismuth (99.997% purity). They had a disc shape of 3 mm height and 10 mm in diameter. For removing defects that occurred during manufacturing and preparation of virgin samples all discs were annealed in the flow of N_2 gas at the temperature of 200°C for 1 h, and then slowly cooled to room temperature. Additionally, they were etched in the 25% solution of nitride acid in distilled water to reduce their thickness by 50 μm and clean their surface. Only one component equal to 0.241 ± 0.001 ns was detected in the measured positron lifetime spectrum for such virgin sample. This value corresponds well with the experimental value reported, i.e. 0.240 ± 0.001 ns. However, for positrons trapped at monovacancy, this lifetime increases to the value of 0.325 ns [12]. The positron lifetime for vacancy cluster one can calculate theoretically.

The results of *ab inition* calculations were carried out using the PAW formalism as implemented in ABINIT code [14, 15]. The positron lifetime computations were performed on 64 atoms of bismuth supercell. A specific supercell was constructed to introduce vacancy around the central atom. The obtained values are depicted in **Figure 2**. For bulk value, the obtained positron lifetime is equal to 0.255 ns and it is slightly higher than the measured value. However, the theoretical value obtained by other authors was about 0.202 ns [12]. The almost linear increase
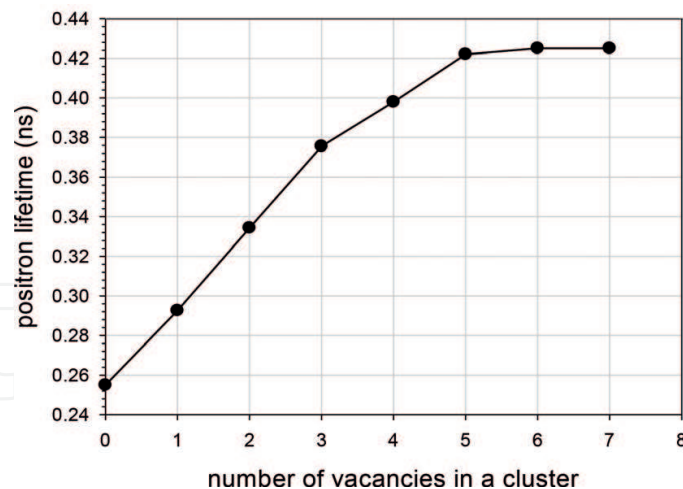
Figure 2. The theoretical values of positron lifetime as a function of the number of vacancies in a cluster of bismuth. The calculation was performed using ABINIT code [15].

of the positron lifetime with the increase of the size of the vacancy cluster is clearly visible, **Figure 2**. However, for the number of vacancies in the cluster larger than five or six this dependency saturates. The obtained results can be helpful in identification of vacancy clusters in the bismuth host.

4. Temperature measurements in bismuth

4.1. Thermally activated monovacancy

For metals, the increase of temperature induces the creation of thermally activated monovacancy. Their concentration increases with the temperature increase. This is reflected also in the temperature increase of the mean positron lifetime (defined below) or values of the S-parameter and hence it can be used for determination of the monovacancy creation enthalpy [16]. The important condition is that the monovacancy must localize positrons. Nevertheless, in the case of bismuth, no increase of the S-parameter with the increasing temperature in the range of 25–200°C is observed, **Figure 3**. The value of the S-parameter remains almost constant indicating lack of positron trapping at thermally activated monovacancy. Similar results were observed not only for bismuth but also for gallium [17] and tin [18]. Thus, the monovacancies in these metals are very weak positron traps because the trapping efficiency rate for such defect must be low. Although $Bi_{40}Sn_{60}$ alloy does not exhibit positron trapping at monovacancies positron trapping at grain boundaries has been observed [19]. The grain boundaries consist of many imperfections including vacancy clusters. Positron trapping at such defects will be shown in the results of the next measurements presented.

4.2. Defects after plastic deformation

In these measurements, bismuth samples were compressed in a flat geometry between two martensitic steel plates using a press with the pressure equal to 3 MPa and the engineering strain
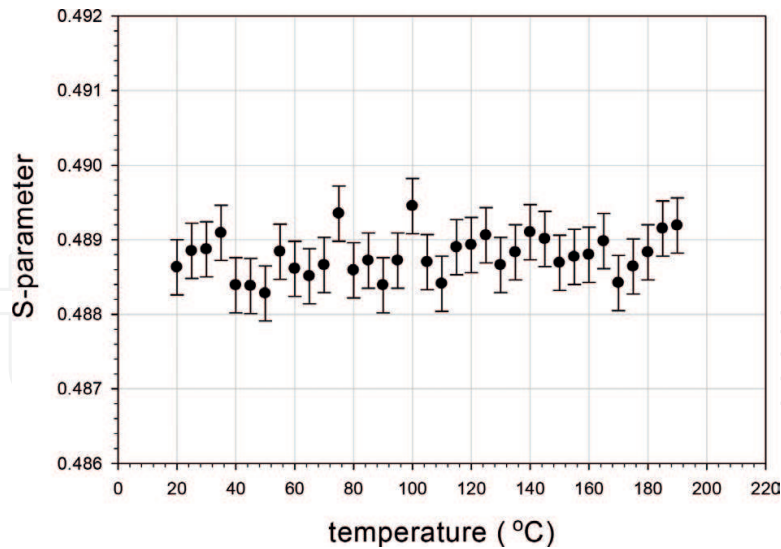
Figure 3. The value of the S-parameter as the function of the temperature obtained in the isochronal annealing measurements for pure bismuth. Each point was measured during 2 h.

equal to 18% [20]. Two components were resolved in the measured positron lifetime spectrum, the value of the first one is equal to 0.178 ± 0.001 ns, the intensity of this component is about (46 ± 5)% and the value of the second one equal to 0.309 ± 0.001 ns the intensity of (54 ± 5)%. Thus, in this process monovacancies or divacancies can be generated, because this value is close to the theoretical values, i.e., 0.293 or 0.334 ns, **Figure 2**. However, the lack of positron trapping at thermally activated monovacancies excludes them.

Creation of such a defect is supported by the fact that the plastic deformation is associated with the movement of dislocations which may cross each other and the jogs on their lines occur. The drag of dislocations with jogs generates monovacancies and interstitial atoms. The latter due to high mobility even at low temperature annihilate with monovacancies. Vacancies are mobile at room temperature too but they can associate creating divacancies or larger clusters. Such a mechanism is commonly accepted. Large vacancy clusters can be presented also at grain boundaries, which are created during the compression in great amount.

For comparison of results obtained for different compression, we apply the commonly accepted robust parameter, i.e., the mean positron lifetime equal to:

$$\overline{\tau} \;=\; \tau_1 I_1 + \tau_2 I_2, \tag{1}$$

where $\tau_{1,2}$ are the positron lifetimes resolved from the positron lifetime spectra and $I_{1,2}$ are their intensities (note: $I_1 + I_2 = 1$). The mean positron lifetime does not depend on the number of components resolved in the positron lifetime spectra, however, it is still sensitive to all parameters corresponding to the annihilation states and properties of the sample at the atomic level. The S-parameter and the mean positron lifetime are complementary parameters.

In **Figure 4**, the dependency of the mean positron lifetime for bismuth samples exposed to compression is depicted [21]. On the x-axis, the thickness reduction or strain of the compressed bismuth samples is indicated. This value increases starting from the bulk value, i.e.,
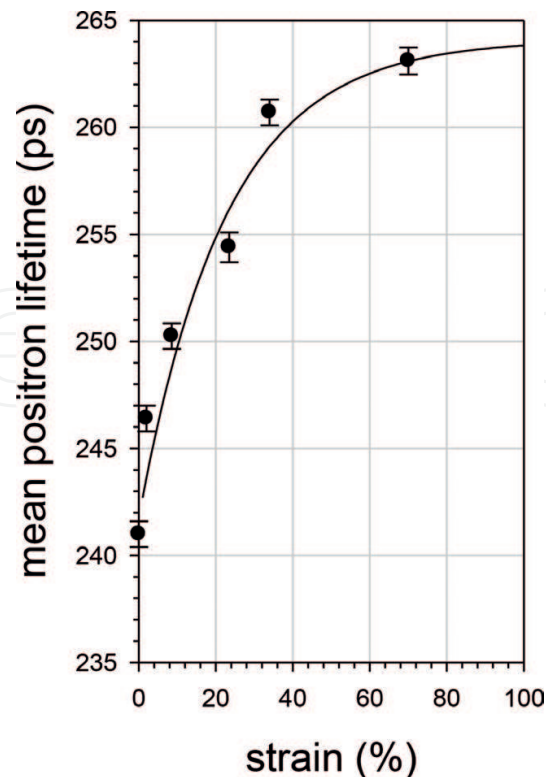
Figure 4. The measured values of the mean positron lifetime vs. thickness reduction or strain of compressed pure bismuth samples [21]. The solid line represents the best fit of Eq. (2), see text.

0.241 ± 0.0006 ns and it saturates at the value of about 0.263 ± 0.0007 ns for the thickness reduction of about 73%. This dependency can be well explained. With the increase in plastic deformation, that is, the increase in stress and strain, a large number of dislocations in shear bands and accompanying them point defects are created. However, at a certain level of defect concentration, all implanted positrons after thermalization and random walk are trapped in these defects. This is reflected in saturation of the positron annihilation characteristics, like mean positron lifetime. Further increase of the deformation and generation of new defects does not affect the positron trapping. This happens at the strain of about 50–60% in bismuth, **Figure 4**. In other metals, saturation occurs already with less deformation about 10% [22].

The obtained dependency in **Figure 4** can be described using a following analytical formula:

$$\bar{\tau} = \tau_{sat} + (\tau_{bulk} - \tau_{sat}) \exp(-c\varepsilon), \tag{2}$$

where ε is the thickness reduction in percent. The solid line in **Figure 4** represents the best fit of this simple function and the values of the adjustable parameters are as follows: τ_{sat} = 0.264 ± 0.003 ns, c = 0.044 ± 0.017.

The obtained value of the bulk lifetime equals to τ_{bulk} = 0.243 ± 0.002 ns. In comparison to other metals, the value of the *c* parameter for bismuth is about one order lower. For instance in copper c = 0.212 ± 0.010 [22]. This can be explained by the fact that in bismuth the mobility of point defects or other defects must be much higher than in copper which melting point is much higher, i.e. 1084°C. This is also clearly visible in the positron lifetime spectra, where for

the highly deformed bismuth sample, the value of the first lifetime is close to the bulk value, i.e., 0.241 ns, which indicates the presence of almost perfect bulk regions. These regions can result from recrystallization process, which can undergo also at room temperature. This can be visible in the following measurements.

4.3. Thermally activated recovery process

The isothermal measurements at room temperature were performed for the bismuth sample after thickness reduction of about 80% in compression. In **Figure 5a**, the obtained dependency of the S-parameter value as the function of time is depicted. The value of the S-parameter decreases and for the time above 10 h, its value ceases decreasing. This indicates that even at room temperature deformed bismuth samples undergo changes at the atomic scale. The recovery and recrystallization process can explain this behavior. This is clearly visible in the isochronal annealing experiment. The bismuth sample after thickness reduction of about 80% was located in the spectrometer, and the value of the S-parameter was measured with the sequenced increase in temperature. Each measurement was done within 2 h, to obtain a suitable accuracy. In **Figure 5b**, the dependency was depicted. Indeed above 40°C, the value of the S-parameter starts gradually decreasing up to the temperature of about 140°C and then saturates. Such a dependency is attributed to the recrystallization process, as we have shown for other metals, i.e., iron, gold or silver [23].
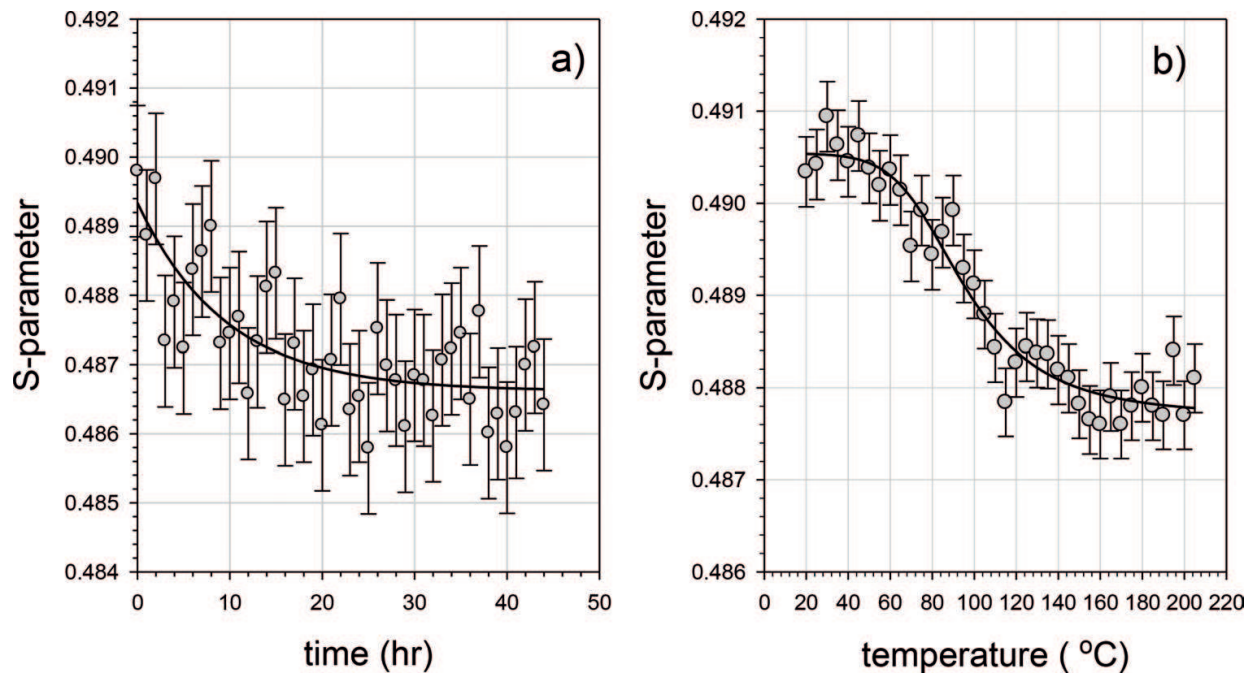

Figure 5. The results of the isothermal measurements of the S-parameter at the room temperature of the bismuth sample after plastic deformation (a). The solid line represents the following function, which is the best fit to the experimental points: $S = 0.486 + \exp(-t/9.5)$, where t is time in hours. The isochronal annealing measurements of the S-parameter for the bismuth samples exposed previously to the plastic deformation (b). The solid line represents the best fit of the function obtained from the positron diffusion trapping model, including the grain boundary migration in the recrystallization process.

The migration of the grain boundaries causes an increase in the size of the new almost defects free grain. Hence, less positrons annihilate at grain boundaries. They contain a great number of defects including vacancy cluster which are traps for positrons. The results from **Figure 5b** can be described within the positron diffusion model, which takes into account not only the positron diffusion but also the model of grain expansion. This allows us to estimate the activation energy for grain boundary migration, which is responsible for this [23]. The solid line in this figure represents the best fit of this model to the experimental points. The obtained value of the grain boundary migration activation energy is equal to Q = 0.84 ± 0.11 eV. We can state that the recrystallization temperature in bismuth is about 90°C, this is the temperature of the middle of the drop of the S-parameter which corresponds the temperature of half-complete recrystallization within a specified time.

5. The subsurface zone in bismuth

The fact that bismuth undergoes recrystallization at room temperature can be reflected in the properties of the subsurface zone generated during dry sliding. To find this the virgin bismuth samples were exposed to dry sliding against the rotating disc made from martensitic steel disc with the speed of about 5 cm/s. In order to obtain the defect depth profile the worn samples were sequentially: etched in a 25% solution of nitride acid in distilled water and after the measurement of positron lifetime spectrum was performed. The layer of about 15 μm thick was removed in every step. The accuracy of a digital micrometer screw used in the thickness measurement was 1 μm.

Two-lifetime components: τ_1 and τ_2 were resolved in each spectrum, and their values as a function of depth from the worn surface are depicted in **Figure 6**. For this sample, the duration of the sliding test was 1 min and applied load was about 10 N. In **Figure 6a**, the mean positron lifetime values are shown. Its value decreases with the increasing depth and exponential decay of this value is clearly visible. This kind of dependency was observed in other metals, e.g. iron [24].

Nevertheless, we have noticed another interesting feature. The value of the first- lifetime component increases and the value of the second-lifetime component remains almost constant with the increasing depth. The explanation can be found in the positron diffusion or standard trapping model [23]. The first-lifetime value lower than the bulk value indicates the fact that the subsurface zone contains almost defects free regions, presumably recrystallized grains. However, the second lifetime, which value is much higher indicates the positron trapping at grain boundaries. The average value of about 0.442 ± 0.058 ns is close to the theoretical value of 0.422 ns for positron trapped at the vacancy cluster which consists of five or more vacancies, **Figure 2**.

Taking into account Eq. (1) which links the strain with the mean positron lifetime, we can calculate the local strain at different depths. The right y-axis in **Figure 6a** represents the results of such calculations. It can be noticed that near the surface, the strain has the value of about 70% and then decay with the depth increase, but even at the depth of 150 μm, it has the value of 5%.
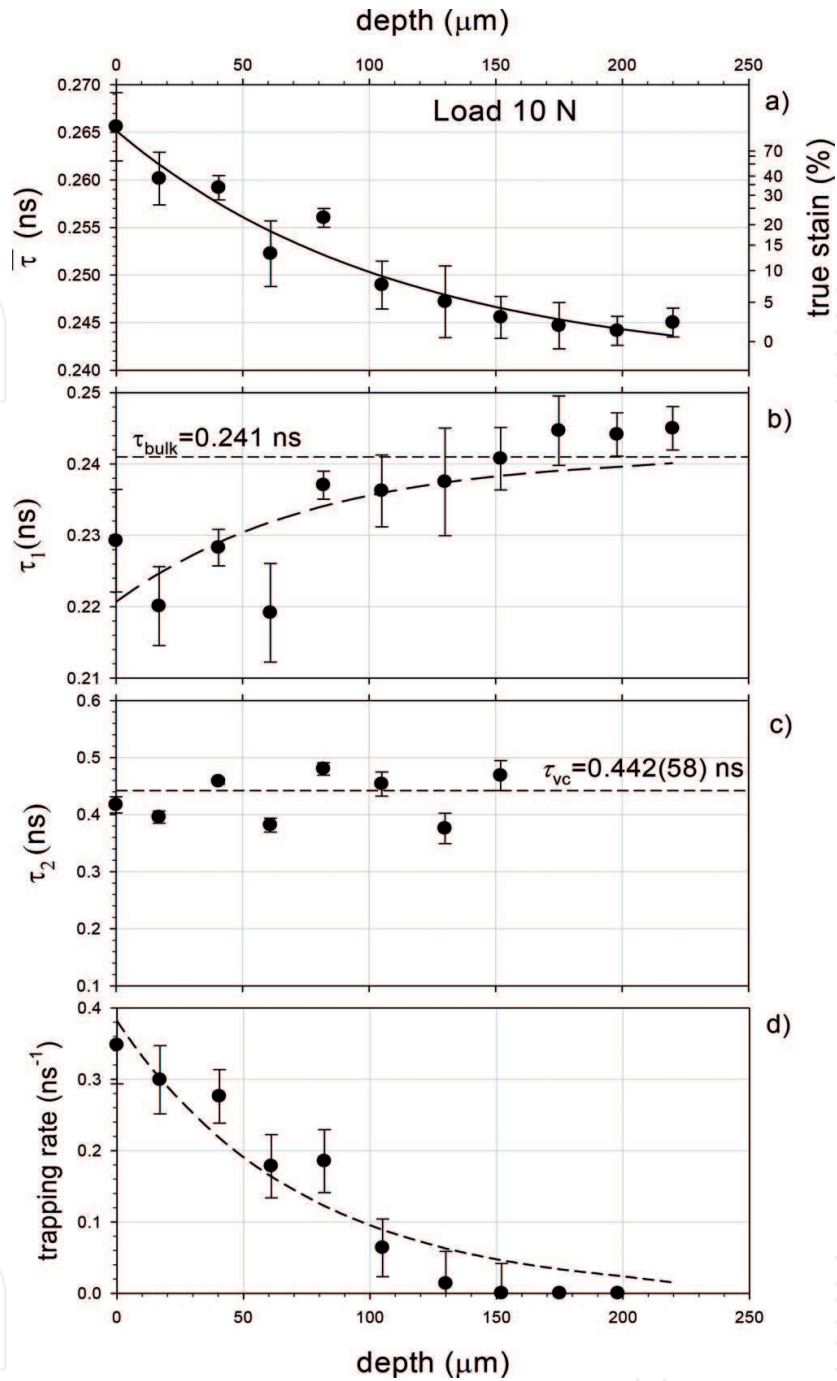
Figure 6. The values of τ_1 (b) and τ_2 (c) resolved from positron lifetime spectra as the function of depth from the worn surface of the sample which was exposed to sliding with the applied normal load equal to 10 N during 1 min [20]. The mean positron lifetime calculated from Eq. (1) and the trapping rate values calculated from Eq. (7) are presented in (a) and (d), respectively. The solid line in (a) and short-dashed line in (d) present the exponential decay functions fitted to the points in each figure. The long-dashed line in (b) presents calculated the value of τ_1 from Eq. (4) taking into account the exponential decay function for the trapping rate, Eq. (8).

To simplify the analysis of the data from **Figure 6**, we use the standard positron trapping model instead of diffusion trapping model mentioned above [10]. It neglects diffusion of positrons but takes into account the trapping at vacancy clusters. In this model, it is assumed that a positron can annihilate from the free state in the bulk or the bound state for instance in the

vacancy cluster where it can be trapped with a certain rate. The average positron lifetime in both states are constant and equal to τ_{bulk} and τ_{vc}, respectively. The transition from the free to the bound state is described by the positron trapping rate which is equal to:

$$\kappa_{vc} = \mu \, C_{vc}, \tag{3}$$

where C_{vc} represents the concentration of the vacancy clusters which bind positrons and μ is the positron trapping efficiency rate. According to this model the first lifetime component in the spectrum is as follows:

$$\tau_1 = \frac{\tau_{bulk}}{1 + \tau_{bulk} \, \kappa_{vc}}, \tag{4}$$

and the second-lifetime component:

$$\tau_2 = \tau_{vc}. \tag{5}$$

The mean positron lifetime is given by:

$$\overline{\tau} = \frac{1 + \tau_{vc} \, \kappa_{vc}}{1 + \tau_{bulk} \, \kappa_{vc}} \, \tau_{bulk}. \tag{6}$$

It is also convenient to express the trapping rate as a function of the mean positron lifetime defined in Eq. (1):

$$\kappa_{vc} = \frac{1}{\tau_{bulk}} \frac{\overline{\tau} - \tau_{bulk}}{\tau_{vc} - \overline{\tau}}. \tag{7}$$

From Eqs. (4) and (5), it is well visible that the increase of the trapping rate and hence the concentration of the vacancy cluster which trap positrons causes the decrease of the first-lifetime component. The second component does not vary.

The average value of the second-lifetime component is 0.442 ± 0.058 ns, **Figure 6c**, and this value corresponds to the annihilation of positrons trapped at a vacancy cluster, which consists more than five vacancies, **Figure 2**. Taking into account the mean positron lifetime Eq. (1) and the average value of the second-lifetime component, we can calculate from Eq. (8) the positron trapping rate as the function of the depth. In **Figure 6d**, we depicted the obtained dependency, which exhibits the exponential decay with the depth increase, represented by a dashed line.

Identical dependencies were observed also for other samples exposed to dry sliding with other values of the applied load, not presented here. The values of the evaluated trapping rate as the function of the depth for various loads applied are depicted in **Figure 7**. For a description of the data from this figure, the following function is proposed:

$$\kappa = b \exp\left(-\frac{d}{d_0}\right), \tag{8}$$

with two b and d_0 adjustable parameters. This function describes well the obtained dependencies. The solid lines in **Figure 7** represent the best fits of Eq. (8) to the experimental points. In **Table 1**, the values of the adjustable parameters are given. It can be stated that with the increasing load the average depth of vacancy cluster distribution, which is represented by the d_0 parameter increases. For the highest load, i.e. 50 N the total depth of the subsurface zone is about 320 ± 20 µm. Like in other pure metals the determined total depth of the subsurface zone is ranged from 140 to 320 µm and it depends on the applied load in the sliding treatment, **Table 1**. The concentration of the vacancy clusters at the worn surface, represented by the b parameter also increases with the applied load.

For determination of the absolute value of the vacancy cluster concentration, the value of the positron trapping efficiency rate: µ, which describes the transition rate from the free to the trapped state is necessary, Eq. (3). This value in metals is ranged from 5×10^{14} to 5×10^{17} s^{-1} [25], however, because of experimental difficulties, it is rarely reported. In turn, the theoretical calculations of this quantity require knowledge about the mechanism of energy transfer from the trapped positron to the host, and this is also difficult to point out it in particular case [26].
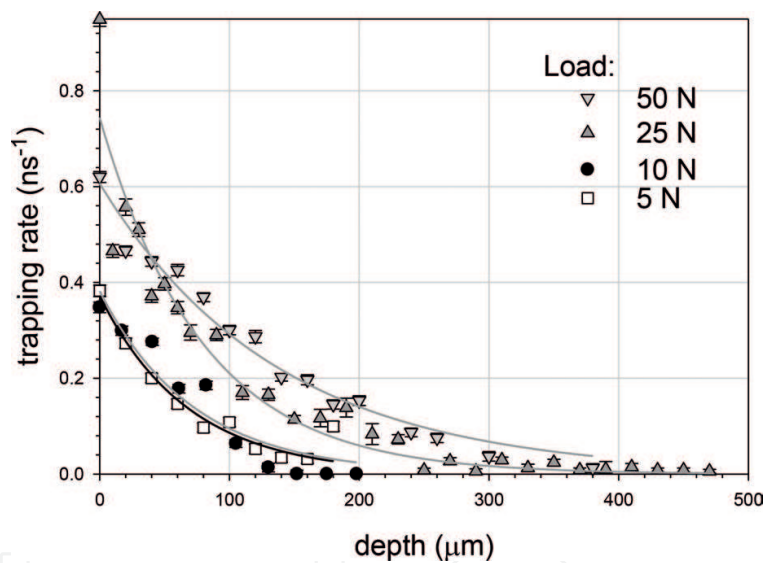

Figure 7. The trapping rate obtained from the positron lifetime spectra, i.e. Eq. (7) as the function of the depth from the worn surface for different loads applied during the test [20]. The tribo test lasted for 1 min for all samples. The solid lines represent the best fit of Eq. (8) to the experimental points, and the adjustable parameters are given in **Table 1**.

Load [N]	d_0 [µm]	b [ns^{-1}]	Total depth of the subsurface zone [µm]
5	68.4 ± 7.5	0.37 ± 0.02	140 ± 20
10	71.9 ± 1.2	0.38 ± 0.04	200 ± 20
25	79.2 ± 7.7	0.74 ± 0.04	280 ± 20
50	136.8 ± 7.7	0.60 ± 0.02	320 ± 20

In the last column, the value of the total depth of the subsurface zone defined as the depth, where the only single value of the positron lifetime equal to the bulk value is resolved.

Table 1. The values of the adjustable parameters from Eq. (8) which was fitted to the experimental points in **Figure 7**, where the trapping rate as a function of depth is depicted [20].

Unfortunately, the lack of data regarding the positron trapping efficiency rate for pure bismuth excludes calculations of the absolute value of the vacancy cluster concentration in the subsurface zone. Nevertheless, we can state that concentration of vacancy clusters decreases exponentially with the depth increase.

6. The workhardening zone in bismuth

The microhardness profile on the cross section of the bismuth sample exposed to dry sliding allows us to detect the workhardening zone. The Vickers microhardness was measured using Zeiss (Neophot 30) microscope at the load of 10 g at different depths from the worn surface.

The only small increase of the microhardness in the layer adjoined the worn surface is observed, **Figure 8**, which only slightly exceeds the error bar. Additionally, the total depth profile is shallower than those detected by positrons, **Figure 7**. The microhardness profile range is less than 150 μm, **Figure 6a**, whereas the range detected by positrons, **Figure 7**, is about 200 μm. This difference can occur as a result of the fact that the microhardness indenter interacts with large regions of the sample in comparison to the atomic scale and is insensitive to the presence of point defects. One should emphasize very week increase of the microhardness in the layer adjoining the worn surface in comparison for example to the case of stainless steel [27] or iron [24]. In the former, the microhardness increases by the factor of about two in comparison to the bulk region. Probably this is the reason that bismuth is not used in frictional junctions, however, recent observations have shown that aluminum alloy containing dispersed bismuth nanoparticles exhibits better wear resistance and frictional properties than aluminum alloy with embedded lead nanoparticles [28]. Both are promising as bearing material.
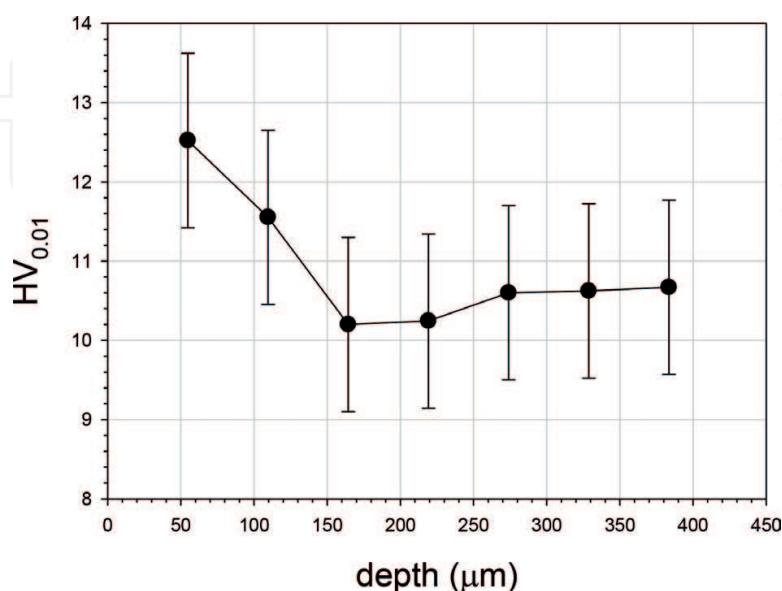

Figure 8. The depth profile of the Vickers microhardness measured on the cross section of the bismuth sample exposed to dry sliding against the rotating disc with the load of 15 N [21].

Acknowledgements

Author details

Jerzy Dryzek

Address all correspondence to: jerzy.dryzek@ifj.edu.pl

Institute of Nuclear Physics PAN, Kraków, Poland

References

[1] Zum Gahr K-H. Microstructure and Wear of Materials. Amsterdam, New York, Tokyo: Oxford, Elsevier; 1987

[2] Horodek P, Dryzek J, Wróbel M. Positron annihilation study of defects induced by various cutting methods in stainless steel grade 304. Tribology Letters. 2012;**45**:341-347. DOI: 10.1007/s11249-011-9890-7

[3] Bowden FP, Tabor D. Friction and Lubrication of Solids. Vol. 2. Oxford, Clarendon Press; 1950

[4] Carbone G, Bottiglione F. Asperity contact theories: Do they predict linearity between contact area and load. Journal of the Mechanics and Physics of Solids. 2008;**56**(8):2555. DOI: 10.1016/j.jmps.2008.03.011

[5] Wert JJ. The role of microstructure in subsurface damage induced by sliding contact. Key Engineering Materials. 1989;**33**:101-134

[6] Dryzek J, Dryzek E, Suzuki T, Yu R. Subsurface zone in pure magnesium studied by positron lifetime spectroscopy. Tribology Letters. 2005;**20**:91-97. DOI: 10.1007/s11249-005-7796-y

[7] Kennedy Jr FE. Plastic analysis of near-surface zones in sliding contacts of metals. Key Engineering Materials. 1989;**33**:35-48

[8] Horodek P, Siemek K, Dryzek J, Wróbel M. Positron annihilation and complementary studies of copper sandblasted at different pressures. Materials. 2017;**10**:1343. DOI: 10.3390/ma10121343

[9] Dryzek J, Horodek P. Positron annihilation studies of the near-surface regionsof niobium before and after wear treatment. Tribology Letters. 2017;**65**:117. DOI: 10.1007/s11249-017-0902-0

[10] Krause-Rehberg R, Leipner HS. Positron Annihilation in Semiconductors. Springer-Verlag; 1999

[11] Yoon H, Sheiretov T, Cusano C. Tribological evaluation of some aluminium-based materials in lubricant/refrigerant mixtures. Wear. 1998;**218**:54-65

[12] Robles JMC, Ogando E, Plazaola FJ. Positron lifetime calculation for the elements of the periodic table. Journal de Physique. 2007;**19**:176222-176220. DOI: 10.1088/1742-6596/265/1/012006

[13] Dryzek J, Singleton D. Implantation profile and linear absorption coefficients for positrons injected in solids from radioactive sources ^{22}Na and ^{68}Ge/^{68}Ga. Nuclear Instruments and Methods in Physics Research Section B. 2006;**252**:197-204. DOI: 10.1016/j.nimb.2006.08.017

[14] Blöchl PE. Projector augmented-wave method. Physical Review B. 1994;**50**:17953-17979

[15] ABINIT code. 2000-2017. Available from: http://www.abinit.org

[16] Triftshauser W. Positron trapping in solid and liquid metals. Physical Review B. 1975;**12**:4634

[17] Szymański C, Chabik S, Pajak J, et al. Temperature-dependence of the positron annihilation in liquid and solid bismuth and gallium. Physica Status Solidi A. 1980;**60**:375-380

[18] Shah N, Catz AL. Temperature dependence of positron annihilation in tin. Physical Review B. 1984;**30**:2498

[19] Chabik S, Rudzińska W, Szuszkiewicz M, et al. Positron annihilation in solid and liquid $Bi_{40}Sn_{60}$ alloy. Acta Physica Polonica A. 1999;**95**:479-482

[20] Dryzek J. Positron studies of subsurface zone created in sliding wear in bismuth. Tribology Letters. 2010;**40**:175-180. DOI: 10.1007/s11249-010-9654-9

[21] Dryzek J. The annealing studies of the subsurface zone induced by friction in bismuth detected by positron lifetime technique. Tribology Letters. 2014;**54**:229-236. DOI: 10.1007/s11249-013-0232-9

[22] Dryzek J, Nojiri S, Fujinami M. The positron microscopy studies of the wear tracks on the copper surface. Tribology Letters. 2014;**56**:101-106. DOI: 10.1007/s11249-014-0389-x

[23] Dryzek J, Wróbel M, Dryzek E. Recrystallization in severely deformed Ag, Au and Fe studied by positron annihilation and XRD method. Physica Status Solidi B. 2016;**253**:2031-2042. DOI 10.1002/pssb.201600280

[24] Dryzek J. Positron studies of subsurface zone in pure iron induced by sliding. Tribology Letters. 2011;**42**:9-15. DOI: 10.1007/s11249-010-9742-x

[25] Schaefer H-E. Investigation of thermal equilibrium vacancies in metals by positron annihilation. Physica Status Solidi A. 1987;**102**:47-65

[26] Dryzek J. Scattering and trapping of positrons at vacancies in solids. Journal of Physics: Condensed Matter. 1995;**7**:L383

[27] Dryzek J, Horodek P, Wróbel M. Use of positron annihilation measurements to detect the defect beneath worn surface of stainless steel 1.4301 (EN) under dry sliding condition. Wear. 2012;**294-295**:264-269. DOI: 10.1016/j.wear.2012.07.006

[28] Bhattacharya V, Chattopadhyay K. Microstructure and tribological behaviour of nano-embedded Al-alloys. Scripta Materialia. 2001;**44**:1677-1682. DOI: 10.1016/S1359-6462(01)00864-8